ANTENNA MODELING BY INFINITESIMAL DIPOLES USING GENETIC ALGORITHMS

T. S. Sijher and A. A. Kishk

Department of Electrical Engineering
Center for Applied Electromagnetic Systems
Research (CAESR), University of Mississippi
University, MS 38677, USA

Abstract—The binary Genetic Algorithm (GA) optimization method is used to simulate antennas from their near-field distribution by a set of infinitesimal dipoles. The infinitesimal dipoles could be of electric and/or magnetic types that produce the near field of the actual antenna and thus the same far field. The method is verified using near fields from known infinitesimal electric and/or magnetic dipoles. Some simple antennas have been simulated by infinitesimal dipoles such as dipole, loop, waveguide, and dielectric resonator antenna. The obtained equivalent dipoles from single frequency measurements are found to be valid for certain frequency band.

1. INTRODUCTION

Measurements of near or far fields from antennas are very expensive and mostly are performed on isolated environments without the effect of the surrounding structures. Study of the actual antennas interaction with the actual structures is, computationally and experimentally, tedious. Also, knowing the far radiated fields, in some plane cuts, of the isolated antenna is not enough for interaction analysis. The simplest radiating element is the infinitesimal dipole that can easily be implemented in any electromagnetic code. An antenna can be simulated by a set of infinitesimal dipoles. Using this set of dipoles replacing the actual antenna can easily be used to compute the radiation from the actual antenna with the presence of the structure because the near and far field in any direction can easily be obtained and used to study the interaction. Also, an unknown radiating antenna can be simulated by a set of dipoles from its known near field distribution and consequently predict its far field radiation patterns in any plane cut. This problem of source identification and then far field prediction from near field measurements has received a lot of attention and a number of different approaches have been studied.

In [1–4] far field is deduced from near-field measurements performed over an arbitrary shaped surface. From measured fields, using the equivalence principle, an equivalent current over the measurement surface is found. Then the far field is computed from these current values. In [5] the far field is determined from the near field using an expression derived from the second Green's identity. In [6, 7] a different approach was adopted. The far field information is computed from near field amplitude only data using phase retrieval algorithms. In [8], a method aimed at the characterization of areas of brain activity is described using another approach. The method is based on the substitution of those areas by dipole sources, which generate the same potential as that measured by an electroencephalograph. The position, magnitude and orientation of the dipoles are found by using Genetic Algorithm. Then later on a similar but modified method for both source identification and far-field radiation prediction from near-field semi anechoic measurements was presented in [10]. The viability of this method, focusing on far-field prediction was first discussed in [9]. The use of the method in [9] was further enhanced with more results in [10]. In [10] more complex DUT were simulated and results from actual measurements were also presented. The method was based on the prediction of an equivalent set of elemental dipoles both magnetic and electric using an optimization routine (Genetic Algorithm), which produces the same near field as the given measured

values, thus modeling the DUT. Once the equivalent set of dipoles has been found, the far field can be easily computed analytically from radiation formulas of the elemental dipoles. In [10] electric field amplitude from semi-anechoic measurements were used.

In this paper the basic approach that has been adopted and used is very similar to the one that was presented in [10]. However a number of modifications and changes were made in the implementation of the method depending upon the different problem in hand. In the prediction of equivalent radiating sources we have used infinitesimal dipoles, and for the sampling points we are considering both the amplitude and the phase of the fields. It is expected that better prediction for the equivalent sources could be obtained. Also the near field data is obtained computationally from analytical solutions and commercial simulation software. Therefore, the near fields are not limited to certain surface. The near field surface can be chosen based on the availability of near field computations of certain software. This is an advantage, since we can use whatever information is available from the near field measurements around the actual source. The solution obtained using this method is then checked for its quality over a range of frequencies and was found to have good bandwidth depending upon the behavior of the actual source with frequency.

2. METHODOLOGY

The problem being discussed above has been implemented in the following strategy:

1. The near field values of the device under test (DUT) are obtained at fixed number of observation points. These are close enough to the source.

2. In order to simulate equivalent dipoles for the given DUT the code is run with random initial values for the characteristics of the dipoles

3. Genetic Algorithm is implemented in the code and the values of dipoles are achieved from optimization using the field measurements at the observation points.

4. If the number of observation points is representative enough, then the right values of equivalents sources can be calculated, which would have the same radiation patterns as the original source.

5. From these values near fields and far field radiation patterns can be obtained.

3. IMPLEMENTATION

An infinitesimal dipole d_i can be characterized by a small number of parameters and therefore makes it suitable for implementation in a code. An infinitesimal dipole i can be described by the following parameters:

- TYPE — There can be two types of dipoles electric or magnetic (type_i)
- MOMENT — To completely describe a dipole in Cartesian coordinates, the dipole moments in x, y, z direction are the complex quantities, Mx_i, My_i, and Mz_i, respectively.
- POSITION — Three quantities x_i, y_i, and z_i, for the dipole position in the Cartesian coordinates.

Therefore, a dipole can be characterized using seven variables

$$d_i = (\text{type}_i, Mx_i, My_i, Mz_i, x_i, y_i, z_i) \tag{1}$$

Notice that the dipole moment in each direction is described by two real values. An integer number 0 or 1 for electric or magnetic type denotes the dipole type, respectively. Therefore, the number of variable describing each dipole is ten and are given in the set d_i as

$$d_i = (\text{type}_i, \text{Re}(Mx_i), \text{Im}(Mx_i), \text{Re}(My_i), \text{Im}(My_i), \\ \text{Re}(Mz_i), \text{Im}(Mz_i), x_i, y_i, z_i) \tag{2}$$

So a set of N radiating dipoles can be represented by $10N$ components vector

$$C = (d_1, d_2, \cdots\cdots, d_N) \tag{3}$$

The vector C is one possible solutions and forms the chromosome. A whole set of different C together forms the entire population for the Genetic Algorithm. Each of the above real variables are binary coded over certain range of interest. For example the dipole positions are chosen to be within the near field box. The real variable is coded in a binary code as $x = b^1 b^2 \cdots b^{Nb}$, where b is 0 or 1 and Nb is the number of bits in the string. The actual variable can be decoded as; $x = x_{\min} + \frac{x_{\max} - x_{\min}}{2^{Nb} - 1} \sum_{i=1}^{Nb} b/2^{(i-1)}$ with $x_{\min}$ and $x_{\max}$ are the minimum and maximum range for the variable x. the variable range and the number of bits are chosen for specific range and resolutions. After optimization for a particular C with the best fitness, it should be the global minima or maxima as desired. The field radiated by the set of

infinitesimal dipoles at a point r_m is a function that depends on all the $10N$ components of the vector C.

$$E(r_m, C) = E(r_m, d_1, d_2, \cdots\cdots, d_N) = \sum_{i=1}^{N} E_i(r_m, d_i) \qquad (4)$$

$$H(r_m, C) = H(r_m, d_1, d_2, \cdots\cdots, d_N) = \sum_{i=1}^{N} H_i(r_m, d_i) \qquad (5)$$

In Equations (4) and (5) E and H are the total fields at r_m and E_i and H_i are the fields at r_m due to particular dipole i. Therefore, any value like the amplitude or phase or just electric field or magnetic field that is measured at r_m will be suitable to recover the vector C that characterizes the dipoles. The larger the number of dipoles, the number of optimization parameters increases, the more challenging and computationally demanding to obtain solution because the requirement of a larger search space increases in order to find the global solution to the problem.

As with any optimization routine the objective function called the fitness function for GA is very important for its good performance. The values that are being predicted through optimization are the different field components. The fitness function was chosen, to take into account all the components of the fields to avoid the needs of the tangential components only, which varies as the coordinate system or the scanning surface changes. In case of actual measurements of the near field which will be only for the tangential fields on the scanned near field surface, only the near field components will be used. The fitness function is taken as

$$F(C) = \sum_{m=1}^{N} \sqrt{ \begin{array}{c} |(Ea_x(m) - E_x(m))|^2 + |(Ea_y(m) - E_y(m))|^2 \\ + |(Ea_z(m) - E_z(m))|^2 \end{array} } \qquad (6)$$

where M is the total number of observation points over the near field scanned surface, Ea_i are the actual field components of the radiating source. The rms error of the electric field is computed as a measure of the fitness as

$$error = \sqrt{ \frac{\sum_{i=1}^{M} |E_{ai} - E_i|^2}{\sum_{i=1}^{M} |E_{ai}|^2} }, \qquad \vec{E} = E_x \hat{x} + E_y \hat{y} + E_z \hat{z} \qquad (7)$$

Table 1. Comparison between test and evaluated equivalent dipoles.

	Type	M_x	M_y	M_z	x(cm)	y(cm)	z(cm)
Actual	Electric	0	0	-5	0	-12.00	0
Predicted	Electric	0.02 +i0.02	-0.32 -i0.16	-5.04 +i0.03	0	-12.0205	0
Actual	Electric	0	-5	0	0	0	0
Predicted	Electric	0.10 -i0.19	-5.07 +i0.02	0.03 +i0.07	0	0	0
Actual	Electric	0	0	5	0	12.00	0
Predicted	Electric	0.03 +i0.02	0.21 -i0.07	5.11 +i0.06	0	12.1500	0

4. RESULTS

The code is verified by reconstructing a set of infinitesimal dipoles
that were chosen arbitrarily in terms of type, position and orientations.
Three dipoles were chosen with moments and position in such a manner
that they represent a loop of current. The actual values of these
parameters and the reconstructed dipoles are given in Table 1. In this
case a population size of 1000 is considered with single point crossover
with probability of 85% and mutation probability of 0.3%. The error
was found to be 3.3%.

The comparisons between the near-fields and far-fields for these
dipoles can be seen in Figures 1 to 4. All of these cases show good
agreement with each other.

Another case of six dipoles is considered. In this case a population
size of 2400 is considered with single point crossover with probability
of 85% and mutation probability of 0.8%. The error was found to be
11.5%. The actual values of these parameters and the ones that have
been obtained from the program can be seen in Table 2.

The comparisons between the near-fields and far-fields for these
dipoles can be seen in Figures 5 to 8. All of these cases show good
agreement with each other.

Actual antennas are also modeled such as half wavelength dipole,
square wire loop, open-end circular waveguide, and a dielectric disc
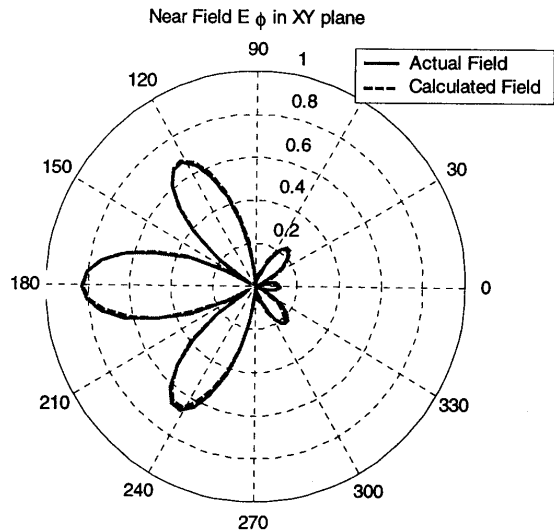antenna. The near-fields are obtained from the method of moments
code WIP-D [11].

Figure 1. Comparison of E_ϕ near field.
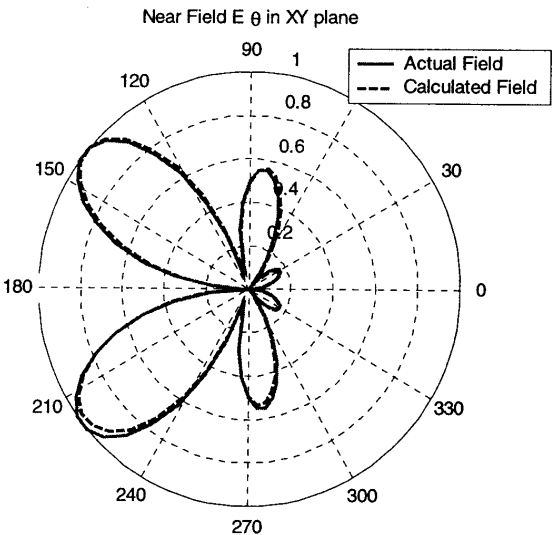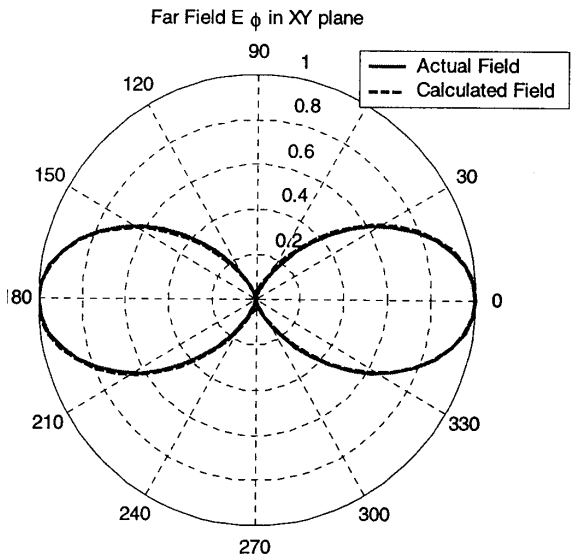

Figure 2. Comparison of E_θ near field.

Far Field E $_\phi$ in XY plane

Figure 3. Comparison of E_ϕ far field.

Far Field E $_\theta$ in XY plane
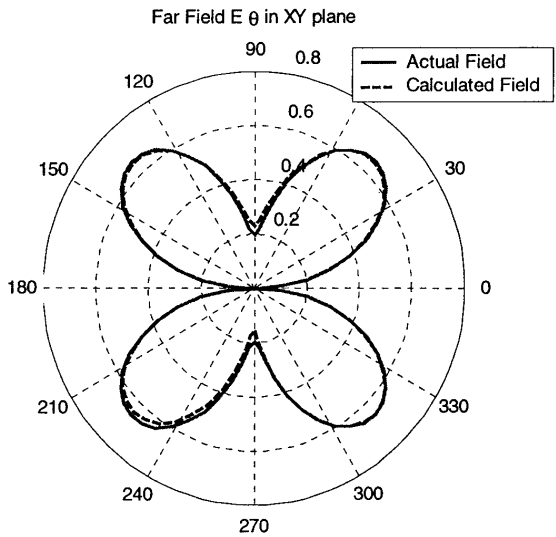
Figure 4. Comparison of E_θ far field.

Table 2. Comparison between test and evaluated equivalent dipoles.

	Type	M_x	M_y	M_z	X (cm)	Y (cm)	Z (cm)
Actual	Electric	0	0	-5	0	-12	0
Calculated	Electric	0.12+j0.27	-1.42+j0.59	-4.6+j0.55	0.78	-13.12	0
Actual	Electric	0	-5	0	0	0	0
Calculated	Electric	-0.37-j0.65	-1.71-j0.42	-0.48+j0	0.07	-0.95	0
Actual	Magnetic	0	0	5	0	12	0
Calculated	Magnetic	0.03+j0.10	1.58-j1.63	4.98+j0.12	-1.25	12.032	0
Actual	Electric	0	0	-5	10	5	0
Calculated	Electric	-0.14+j0.83	-1.84-j0.95	-5.68+j0.33	9.54	4.46	0
Actual	Electric	-5	0	0	0	0	0
Calculated	Electric	-4.95-j0.29	-0.47+j1.31	-0.36-j1.02	0.47	-0.59	0
Actual	Magnetic	0	0	5	10	5	0
Calculated	Magnetic	-1.98-j2.59	1.31-j0.59	4.82+j0.48	10.68	5.7795	0

Figure 5. Comparison of E_ϕ near field.

Near Field E θ in XY plane
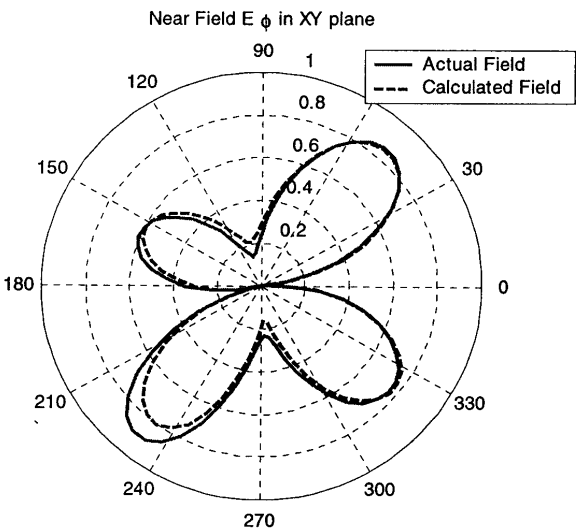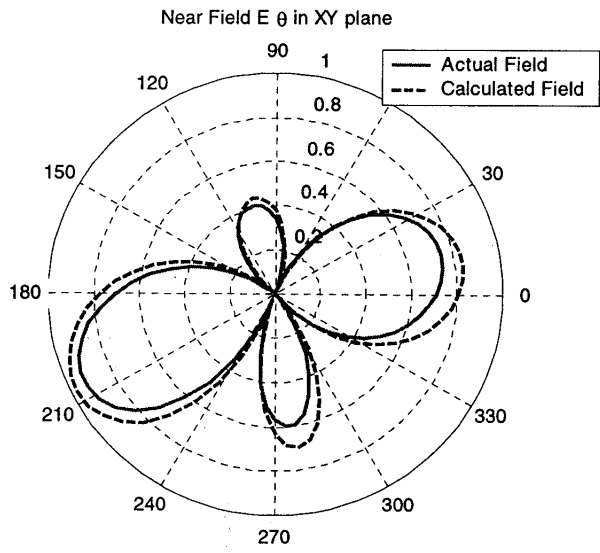
Figure 6. Comparison of E_θ near field.

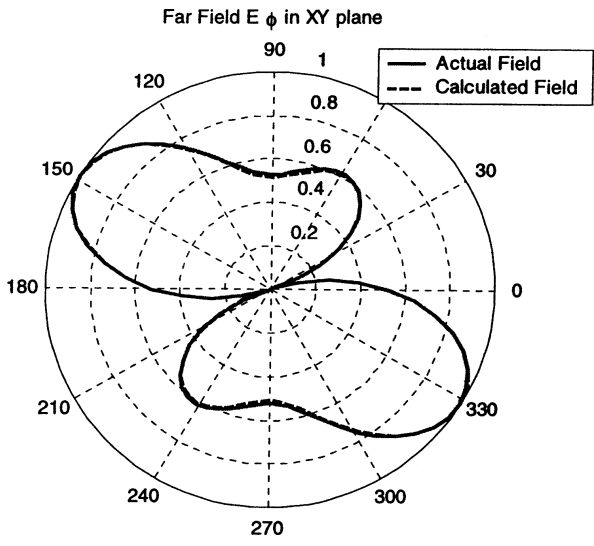Far Field E ϕ in XY plane

Figure 7. Comparison of E_ϕ far field.
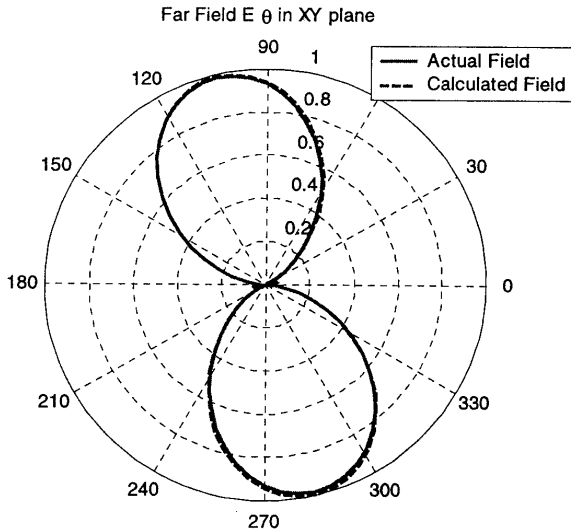
Figure 8. Comparison of E_θ far field.

4.1. Wire Dipole Antenna

A half wavelength dipole antenna oriented along the z-axis is considered. The wire radius is very small compared to its length. The antenna is center fed by a source with frequency of 300 MHz. The sampling points of the near field were on a cube enclosing the dipole. The side of the box was of the order of 0.8λ. The size of the box is an important parameter to be chosen. It should not be very close to the antenna or very far to avoid the rapid variations of the field or to lose some information in the far field, respectively. A box of side length of 0.8λ was found to be optimum for the dipole antenna after doing a number of simulations for different values. Table 3 shows the equivalent dipoles obtained to simulate this antennas. The rms error is found to be about 2.35%. It was expected that all the dipoles be z-directed and spanning over a longer distance, the results show that the dipoles have not been symmetrically arranged. It seems that the unexpected dipole moments and orientations have compensated to certain degree such a need for the symmetry. Results from the above set of dipoles are shown in Fig. 9 for the near fields at contour line through the yz-plane indicating good agreement between the actual field and the simulated fields. For better understanding, Fig. 10 shows the plane cut with the comer coordinates marked. The corners are also marked with a node numbers corresponding to the observation points corresponding to the

Table 3. Five equivalent dipoles for half wave length dipole.

	Type	M_x	M_y	M_z	x(cm)	y(cm)	z(cm)
1	Electric	36.4173 +j8.8583	-26.5748 -j24.6063	121.0630 -j79.7244	0.1181	-0.8268	-16.7323
2	Electric	-36.4173 -j34.4488	14.7638 +j34.4488	119.0945 -j87.5984	-0.4331	-1.2205	-1.7717
3	Electric	24.6063 +j42.3228	-0.9843 -j18.7008	117.1260 -j97.4409	-0.9055	-0.1181	13.9764
4	Electric	-22.6378 +j48.2283	26.5748 +j10.8268	125.0000 -j77.7559	0.3543	0.5118	-2.5591
5	Electric	14.7638 -j58.0709	-22.6378 -j8.8583	107.2835 -j40.3543	-0.5906	1.9291	9.2520

(a)   (b)
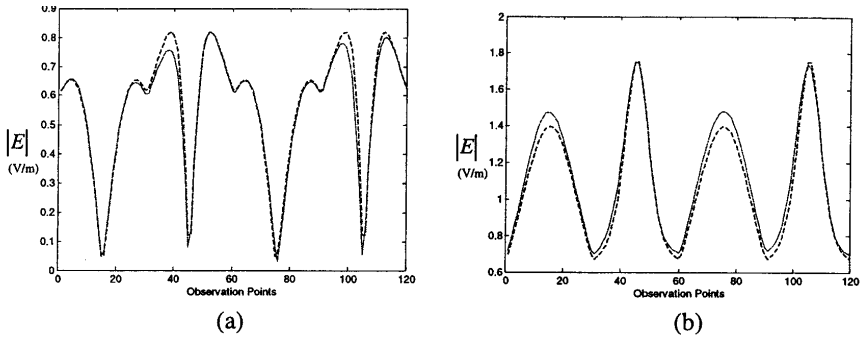
Figure 9. Near-field of $\lambda/2$ dipole antenna at $300\,\text{MHz}$, (solid line for equivalent dipoles and dashed lines for actual antenna) (a) Ex, (b) Ez.

electric field plots.

The frequency response of the equivalent dipoles is compared with frequency response of the actual dipole as shown in Fig. 11 at the frequencies 200 and 400 MHz, respectively. The validity of the frequency band will depend on the frequency band of the excited mode at the tested frequency. For example, as far as the current distribution on the dipole does not change its behavior with the frequency, the equivalent dipole could be valid, but if the current distribution changes as the case when the frequency increases to that makes the dipole close or larger than one wavelength, the frequency response will be out of the frequency range of the measured mode. The rms errors for 200 MHz and 400 MHz were found to be 2.1% and 2.8% respectively.
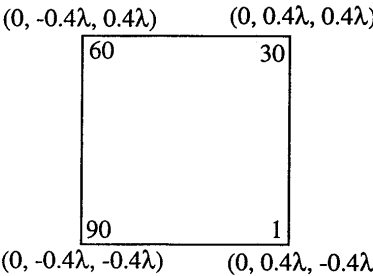
(0, -0.4λ, 0.4λ)   (0, 0.4λ, 0.4λ)

```
60                    30




90                     1
```

(0, -0.4λ, -0.4λ)   (0, 0.4λ, -0.4λ)

Figure 10. Coordinates of the near field plane cut.

Table 4. Equivalent set of dipoles simulating the square loop wire antenna.

	Type	M_x	M_y	M_z	x(cm)	y(cm)	z(cm)
1	Electric	30.5118 -j12.7953	-14.7638 -j8.8583	32.4803 -j26.5748	0.3543	1.9291	0.1969
2	Electric	6.8898 +j24.6063	18.7008 +j30.5118	-4.9213 -j6.8898	0.8268	1.0630	0.1181
3	Electric	-2.9528 -j16.7323	2.9528 +j8.8583	-52.1654 +j0.9843	0.4331	2.0866	0.5906
4	Electric	-34.4488 +j4.9213	-6.8898 -j28.5433	24.6063 +j32.4803	0.1969	1.1417	0.5118

4.2. Square Loop Wire Antenna

A square loop antenna of a 0.05λ side length is considered. The antenna is on the XY plane with its center at the origin. Thickness of wire is much smaller than the side length of the wire. The antenna is fed at the center of one side by a source excited at 300 MHz. The numerical results are obtained using WIP-D. The near field is scanned on a cube surrounding the loop of side length of 0.8λ. Four equivalent dipoles are used to simulate the loop antenna. The parameters of the equivalent dipoles are given in Table 2. The rms error is computed and found to be 4.63%. Again, we can observe that the dipole moments and positions do not follow what would be expected for these dipoles.

Fig. 12 shows the comparisons of the three components of the electric field in the near field on a closed contour on the yz-plane. The near field is plotted on the same plane cut as shown in Fig. 10. These figures show very good agreement between the actual filed and the field
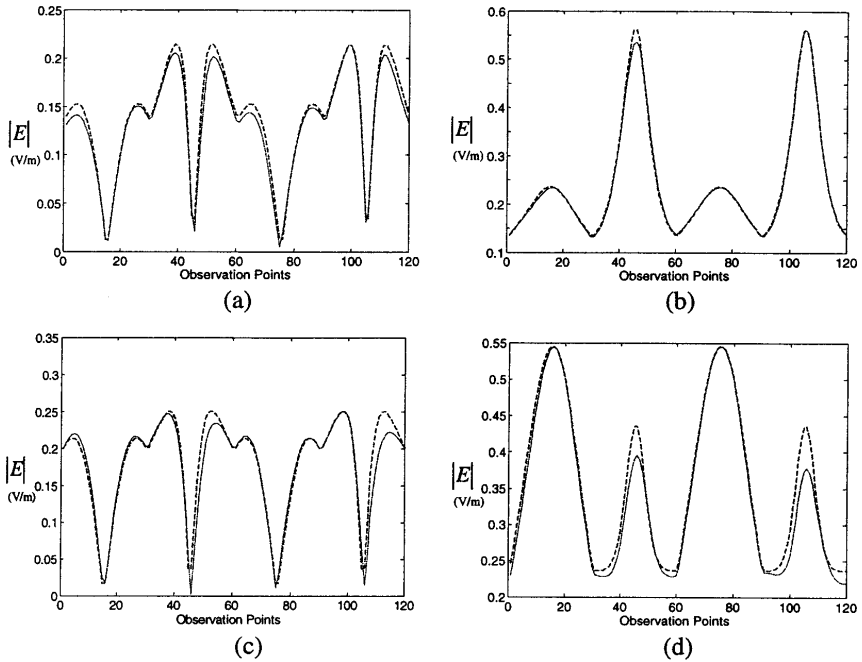
Figure 11. Near-field of the half wavelength dipole antenna at different frequencies, (solid line for equivalent dipoles and dashed lines for actual antenna) (a) Ex (200 MHz) (b) Ez (200 MHz), (c) Ex, (400 MHz) (d) Ez (400 MHz)

from the equivalent dipoles.

The equivalent set of dipoles was tested for there quality over a range of frequencies. Results have been presented in Fig. 13 showing the different components of the electric field along an outline of the cube surrounding the antenna for two frequencies. RMS errors were found to be 5.1% and 4.87% for the frequencies 250 MHz and 350 MHz, respectively. Good agreement of near field shows that the equivalent dipoles have a valid operating bandwidth of 33%.

4.3. Radiating Circular Waveguide

A circular waveguide of finite length is considered. The waveguide is short circuited from one end and opened from the other end and is excited by a dipole located inside on the waveguide axis and oriented in the y-direction to excite the TE_{11} mode. The dipole
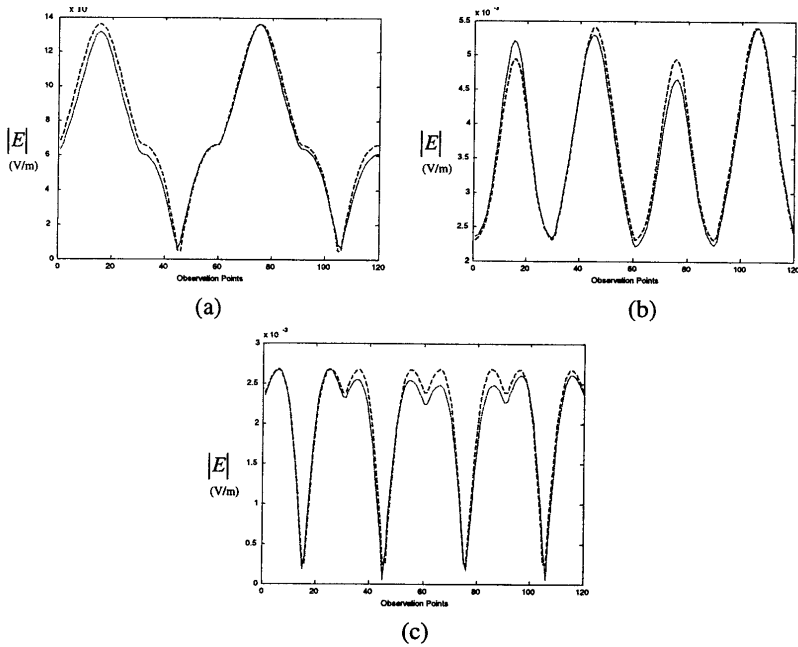
Figure 12. Near-field of the square loop antenna at 300 MHz, (solid line for equivalent dipoles and dashed lines for actual antenna) (a) Ex, (b) Ey, (c) Ez.

position and orientation will not excite the zero order modes. Cut-off frequency for TE_{11} mode was found to be 7.3 GHz and TM_{11} mode was 15.25 GHz. Bandwidth for TE_{11} mode was found to be 1.6588:1. Detailed dimensions of the waveguide can be seen in Fig. 14. The antenna is operated at 10 GHz. This antenna is simulated by five dipoles. The near field box was taken as a cube surrounding the antenna and the bottom side was ignored. The parameters of the equivalent sets of dipoles are given in Table 5. This set of dipoles has a 7.1% rms error.

The near field on the intersection line between the near field box and the yz-plane is given in Fig. 15. The coordinates of this outline are shown in Fig. 16. The x-component that represents the cross polarization is ignored because it is very weak and found to be in the order of 10^{-9} as compared to the other field components.

The frequency response of the equivalent dipoles is also considered. The near-field results at 9 GHz and 12.5 GHz are given in Fig. 17. RMS errors for these frequencies were 7.4% and 7.9% respectively.
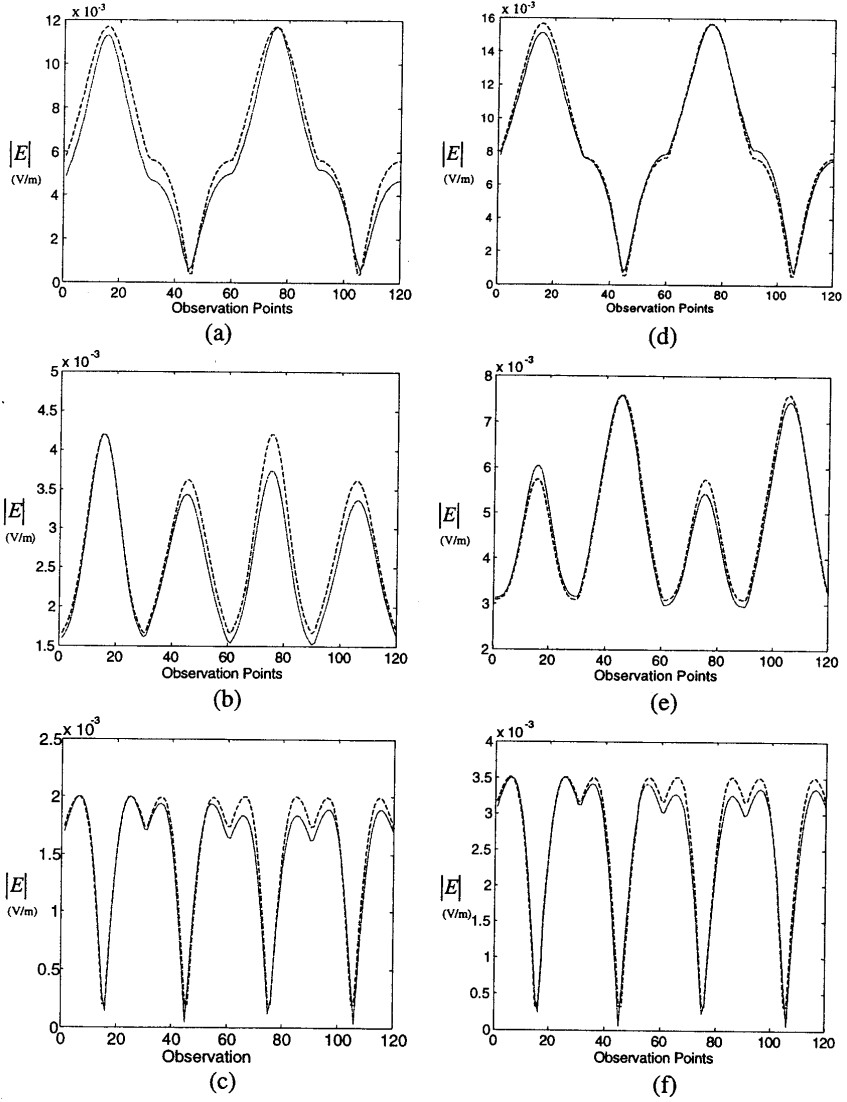
Figure 13. Near-field of the square loop antenna at different frequencies, (Solid line for equivalent dipoles and dashed lines for actual antenna) (a) Ex (250 MHz), (b) Ey (25C MHz), (c) Ez (250 MHz), (d) Ex (350 MHz), (e) Ey (350 MHz), (f) Ez (350 MHz).
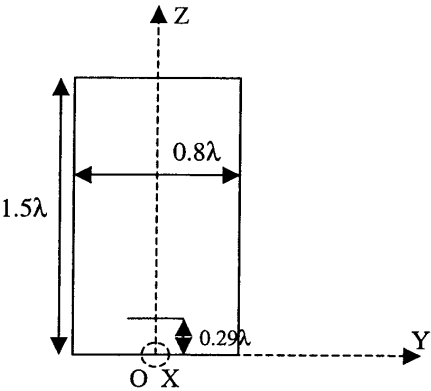
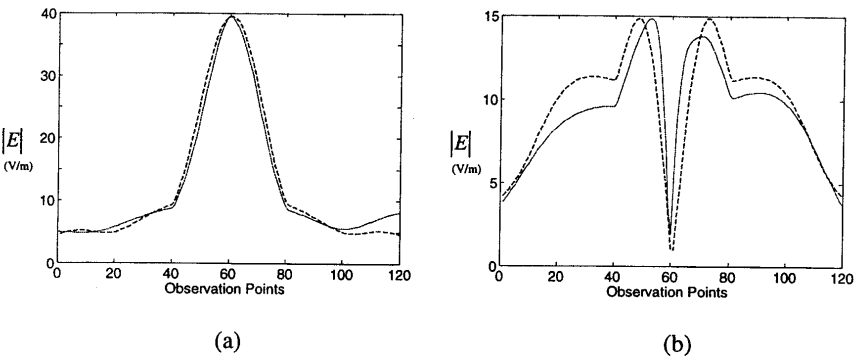**Figure 14.** Dimensions of the waveguide.

(a)   (b)

Figure 15. Near-field of circular waveguide antenna at $10\,\mathrm{GHz}$, (solid line for equivalent dipoles and dashed lines for actual antenna) (a) Ey, (b) Ez.
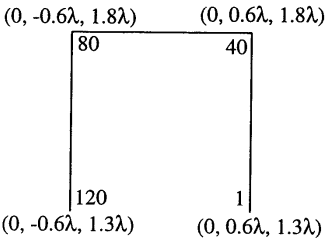

Figure 16. Coordinates of the near field plane cut for cylindrical waveguide aperture.
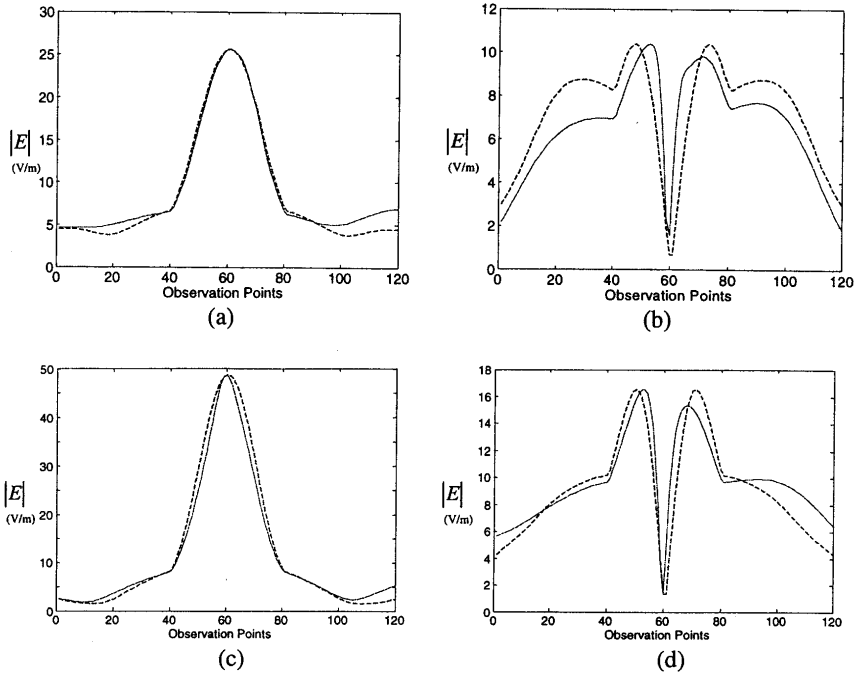
Figure 17. Near-field of the waveguide antenna at different frequencies, (solid line for equivalent dipoles and dashed lines for actual antenna) (a) Ey (9 GHz), (b) Ez (9 GHz), (c) Ey (12.5 GHz), (d) Ez (12.5 GHz).
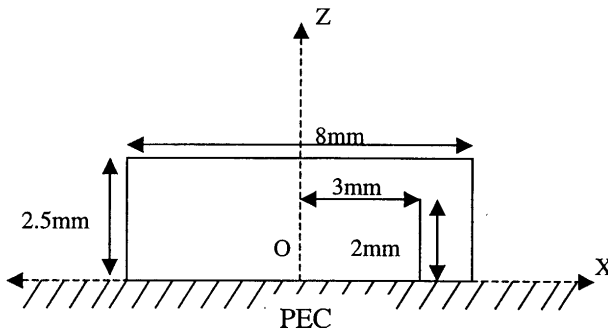

Figure 18. Dimensions of the dielectric resonator antenna with ground plane.
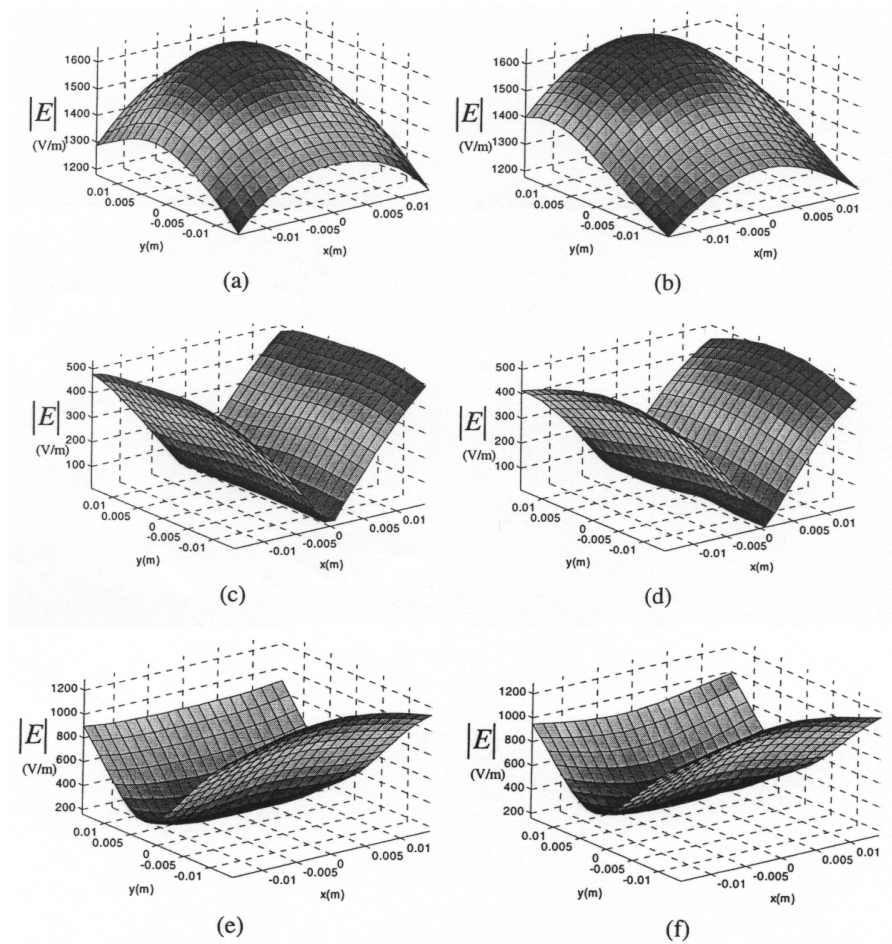
Figure 19. Near-field of the DRA and the equivalent dipoles on a plane $z = \lambda$ above the ground plane. The left side (a), (c) and (e) are for Ex, Ey and Ez for DRA and right side (b), (d) and (f) are their corresponding for the equivalent dipoles.
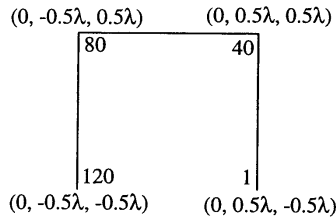
(0, -0.5λ, 0.5λ)   (0, 0.5λ, 0.5λ)

80   40

120   1
(0, -0.5λ, -0.5λ)   (0, 0.5λ, -0.5λ)

Figure 20. Coordinates of the near field plane cut for DRA.

Table 5. Five equivalent dipoles for waveguide aperture.

	Type	Mx	My	Mz	x(cm)	y(cm)	z(cm)
1	Electric	-26.7874-j26.7874	-122.0315 -j62.5039	-0.9921 +j70.4409	0.5575	-0.7465	4.2724
2	Electric	4.9606 +j4.9606	-80.3622 +j126.000	0.9921- j4.9606	-0.0284	0.0850	4.7095
3	Electric	16.8661+j 26.7874	-122.0315 -j122.031	-0.9921 -j32.7402	0.8409	0.3874	4.1780
4	Electric	-20.8346 -j40.6772	-110.1260 -j124.015	6.9449 -j64.4882	-0.4441	0.5953	4.0598
5	Electric	20.8346 +j28.7717	-126.000 -j106.157	-4.9606 +j46.6299	-0.7654	-0.4441	4.2016

Table 6. Five equivalent dipoles simulating the dielectric resonator antenna.

|	Type	Mx	My	Mz	x (mm)	y (mm)	z (mm)
1	Electric	-32.9606 -j34.5039	-0.5512 -j3.6378	39.5748 +j16.4252	-1.9055	7.1811	0.1417
2	Electric	5.6220 +j36.4882	-59.1969 +j24.1417	-5.1811 +j44.2047	0.6142	5.0709	1.9370
3	Electric	24.1417 -j37.5906	28.7717 +j10.2520	8.7087 -j2.0945	1.6850	7.0551	0.2520
4	Electric	2.5354 -j6.7244	-17.5276 -j26.7874	10.2520 +j11.7953	1.4961	4.0630	0.1575
5	Electric	7.1654 +j41.1181	47.2913 +j5.6220	44.2047 -j22.1575	0.4252	8.0000	0
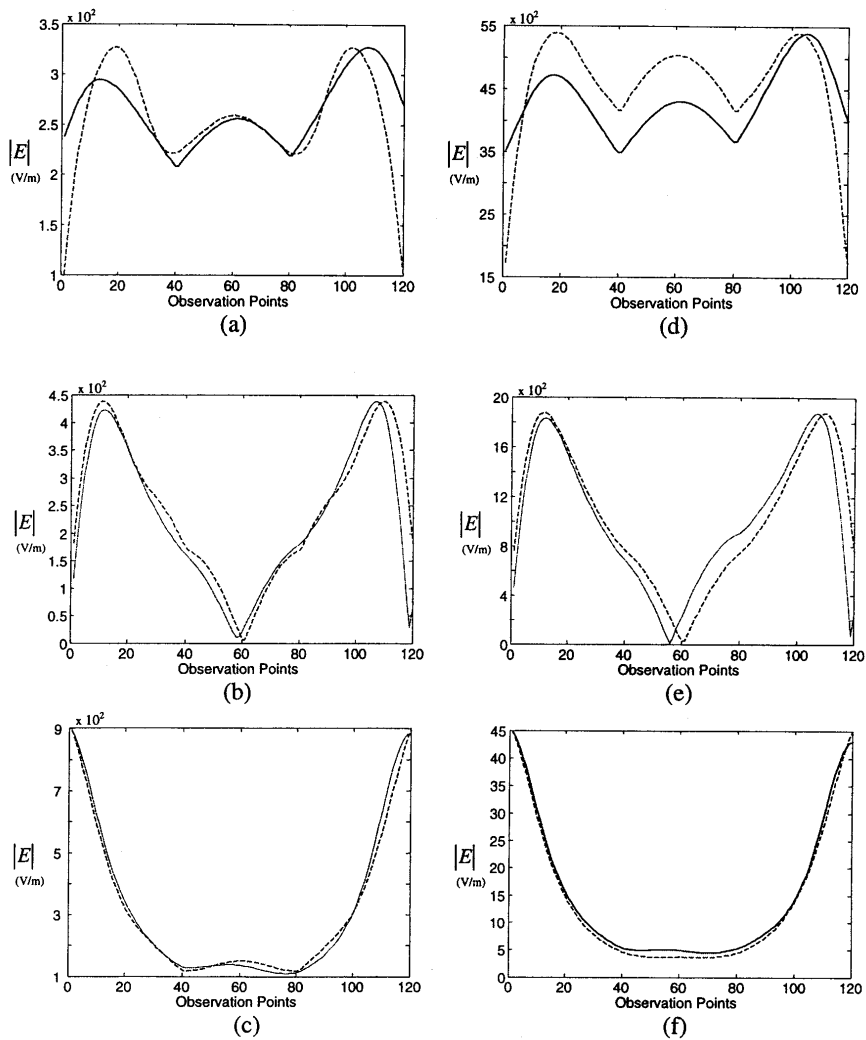
Figure 21. Near-field of the DRA and the equivalent dipoles at different frequencies, (solid line for equivalent dipoles and dashed lines for actual antenna) (a) Ex (8.5 GHz), (b) Ey (8.5 GHz), (c) Ez (8.5 GHz), (d) Ex (11.5 GHz), (e) Ey (11.5 GHz), (f) Ez (11.5 GHz).
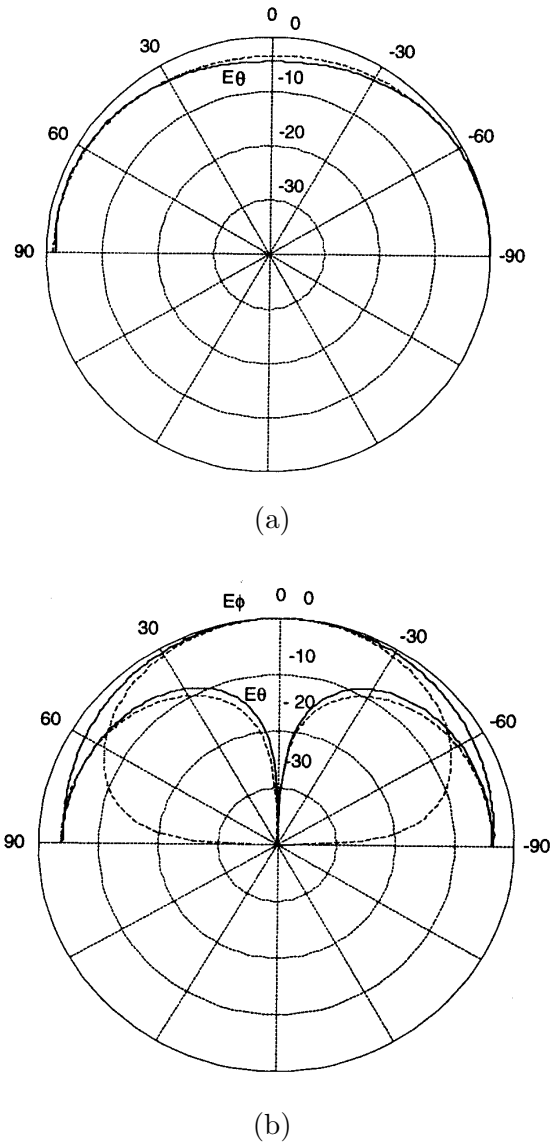
(a)

(b)

Figure 22. (a) E-plane, (b) H-plane and cross-polarization for the DRA above infinite ground plane compared to their corresponding from the equivalent dipoles at 10 GHz (solid line for equivalent dipoles and dashed lines for actual antenna).
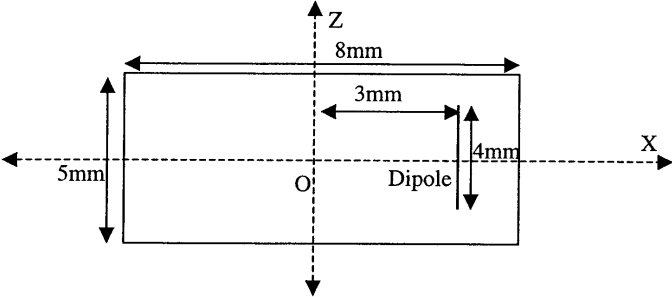
Figure 23. Dimensions of the dielectric resonator antenna.

Table 7. Five equivalent dipoles for dielectric resonator antenna without ground plane.

	Type	Mx	My	Mz	x (mm)	y (mm)	z (mm)
1	Electric	-10.9134 -j0.9921	0.9921 +j2.9764	0.9921 -j84.3307	-5.2756	-0.2362	0.2362
2	Electric	-14.8819 -j88.2992	0.9921 -j6.9449	4.9606 +j16.8661	0.3937	-0.2362	5.7480
3	Electric	-26.7874 -j62.5039	6.9449 +j12.8976	38.6929 +j126.000	6.3780	0.2362	1.3386
4	Electric	18.8504 +j86.3150	-20.834 -j10.9134	14.8819 +j86.3150	4.6457	-0.3937	-2.7559
5	Electric	32.7402 +j50.5984	18.8504 +j0.9921	8.9291 +j6.9449	1.0236	0.7087	-4.8031

4.4. Dielectric Resonator Antenna with Ground Plane (DRA)

A dielectric resonator antenna disc is considered. The disc is located on an infinite ground plane and excited by a coaxial probe normal; to the ground plane and housed inside the dielectric disc off its axis. Detailed dimensions of the antenna are given in Fig. 18; the dielectric constant of the disc is 10.2. Five equivalent dipoles are considered to simulate the antenna. The RMS error is found to be 7.52%. The parameters of the equivalent dipoles are given in Table 6.

The near field of the actual antenna and that of the equivalent dipoles are computed on the plane $z = \lambda$. A total of 400 observation points are computed on a square area as shown in Fig. 19. This case
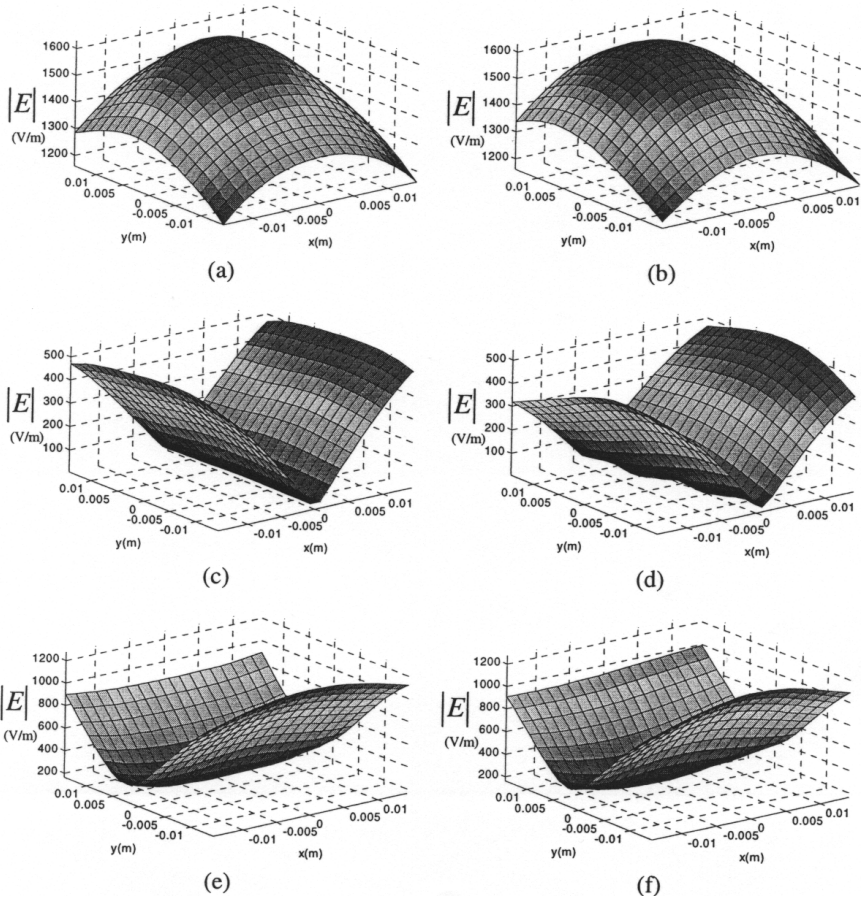
Figure 24. Near-field of the imaged DRA and the equivalent dipoles
on a plane $z = \lambda$ from the image plane. The left side (a), (c) and (e)
are for Ex, Ey and Ez for DRA and right side (b), (d) & (f) are their
corresponding for the equivalent dipoles.

was modeled at a frequency of 10 GHz The similarity between the near
field from the actual antenna and the equivalent set of dipoles is clear.

The frequency response is also computed and found that the
equivalent set of dipoles provides a 30% valid bandwidth.   The
coordinates of the line cut on the xz-plane are shown in Fig. 20. The
near electric field on the cut is shown in Fig. 21 for 8.5 and 11.5 GHz,
respectively. The RMS errors at these frequencies are 7.63% and 8.2%
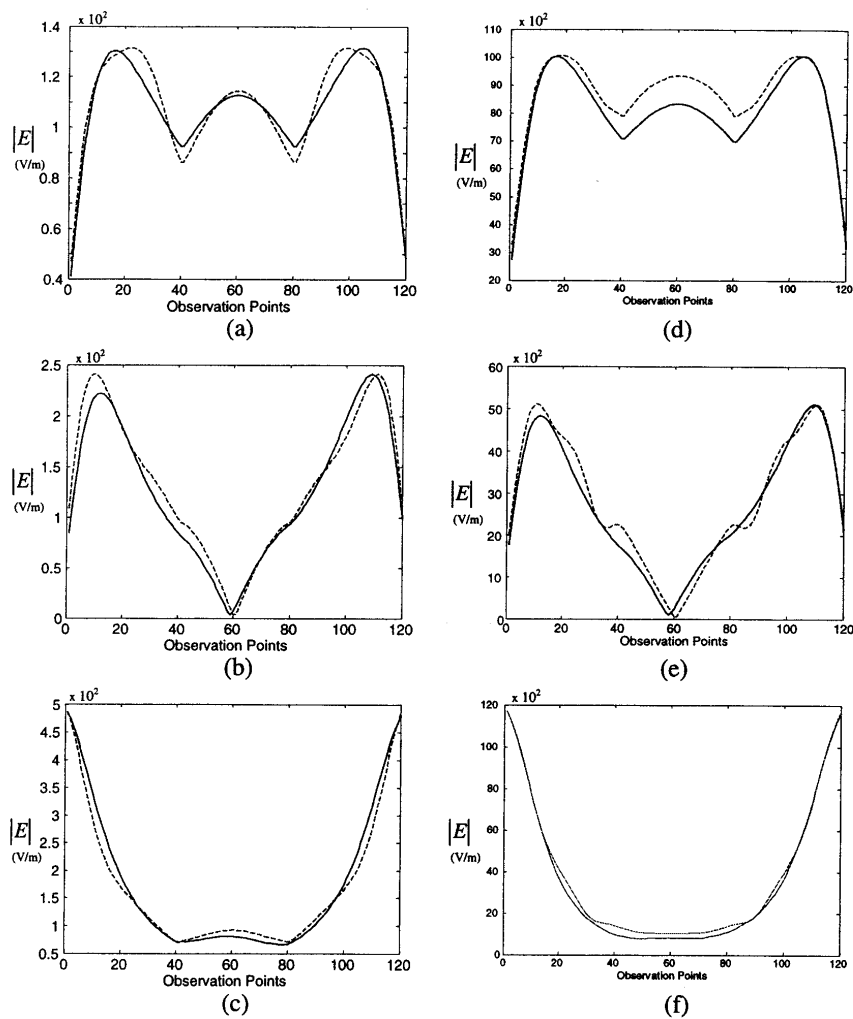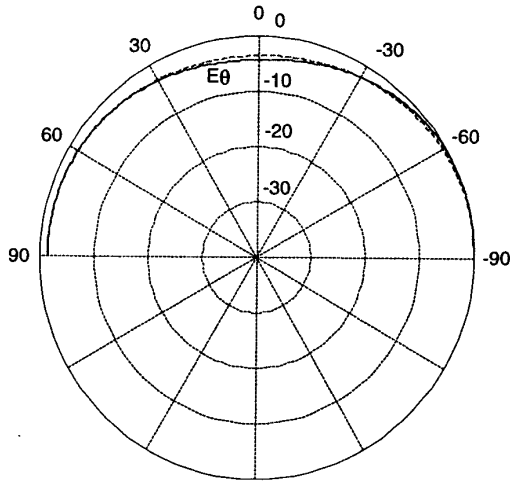respectively.
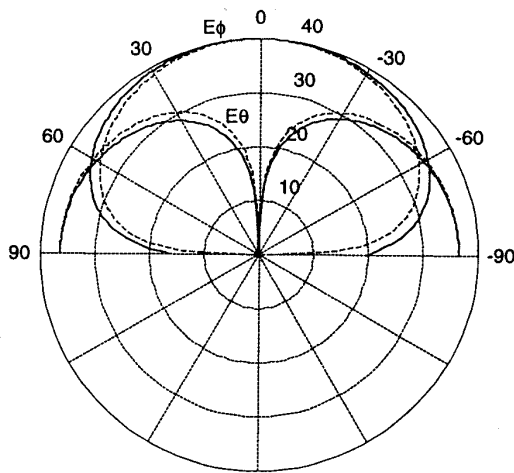
Figure 25. Near-field of the DRA and the equivalent dipoles at different frequencies, (solid line for equivalent dipoles and dashed lines for actual antenna) (a) Ex, (b) Ey, (c) Ez (7.5 GHz), (d) Ex, (e) Ey, (f) Ez (11 GHz).

(a)

(b)

Figure 26. (a) *E*-plane, (b) *H*-plane and cross-polarization for the DRA without infinite ground plane compared to their corresponding from the equivalent dipoles at 10 GHz (solid line for equivalent dipoles and dashed lines for actual antenna).

Far Field Comparison: Far Fields are computed for the DRA as shown in Fig. 22. Fig. 22a shows the far field in the E-plane and it shows very good agreement with the actual case. It can be seen that in Fig. 22b , the H-plane is zero on the infinite ground plane, but the equivalent dipoles did not achieve that. The actual antenna considers the presence of the infinite ground plane, but the dipoles uses the free space Green's function. Therefore, it couldn't achieve this behavior for the far filed in this direction.

5. DIELECTRIC RESONATOR ANTENNA WITHOUT GROUND PLANE

The dielectric resonator antenna modeled in this case is same as the one presented in previous section, but image theory is used to remove the infinite ground plane. The near field sampling points in this case were taken on a cube, which enclosed the entire antenna. The purpose of modeling this case is to see if the presence of ground plane in the previous case made an effect on the quality of the far field results. Detailed dimensions of the antenna are given in Fig. 23; the dielectric constant of the disc is 10.2. Five equivalent dipoles are considered to simulate the antenna. The RMS error is found to be 7.15%. The parameters of the equivalent dipoles are given in Table 7.

The near field of the actual antenna and that of the equivalent dipoles are computed on the plane $z = \lambda$. A total of 400 observation points are computed on a square area as shown in Fig. 24. This case was modeled at a frequency of 10 GHz The similarity between the near field from the actual antenna and the equivalent set of dipoles is clear.

The frequency response is also computed and found that the equivalent set of dipoles provides a 35% valid bandwidth. The near electric field in a cut of the near-field box is plotted as shown in Fig. 25 for 7.5 and 11 GHz, respectively. The RMS errors for at these frequencies are 7.23% and 8.1% respectively. The details of the cut can be seen in Fig. 20.

Far Field Comparison: Far Fields computed for the DRA are shown in Fig. 26. Fig. 26a shows the far field in E-plane, it shows very good agreement with the actual case. In Fig. 26b the far field comparisons for H-plane are shown. It is clearly observed that in this case the H-plane fields agree much better than previous case, thus validating our explanation given in the case of DRA above infinite ground plane.

6. CONCLUSION

An interesting and effective method for the prediction of both near and far field was presented, which was tested with different antenna types. This method is based on the substitution of the original radiating source by a set of infinitesimal dipoles, which produce the same near field as the original source. Infinitesimal dipoles are a good choice for this application because they are the simplest form of radiators with simple mathematical expressions for both near and far fields. The characteristics of these dipoles are evaluated using the Genetic Algorithm as the optimization method. The GA optimizes the parameters of the equivalent dipoles to obtain near fields from them as close to the original antenna as possible. This method was found to be very suitable since it's a global optimization method, which doesn't require initial solution. Using this method solution for antennas were obtained at a particular frequency. These dipoles were found to have similar behavior to the actual antenna with in certain frequency band. Results for near field comparisons on a plane and also far field comparisons have been presented for the DRA.

REFERENCES

1. Petre, P. and T. K. Sakar, "Planar near-field to far-field transformation using an equivalent magnetic current approach," *IEEE Transactions on Antennas and Propagation,* Vol. 40, 1348–1356, November 1992.
2. Petre, P. and T. K. Sakar, "Planar near-field to far-field transformation using an array of dipole probes," *IEEE Transactions on Antennas and Propagation,* Vol. 42, No. 4, 534–537, April 1994.
3. Sakar, T. K. and A. Taaghol, "Near-field to near/far-field transformation for arbitrary near-field geometry utilizing an equivalent electric current and MoM," *IEEE Transactions on Antennas and Propagation,* Vol. 47, 566–573, March 1999.
4. Taagol, A. and T. K. Sakar, "Near-field to near/far-field geometry,

utilizing an equivalent magnetic current," *IEEE Transaction on Electromagnetic Compatability,* Vol. 38, 536–542, August 1996.

5. Laroussiand, R. and G. I. Costache, "Far-field predictions from near-field measurements using an exact integral equation solution," *IEEE Transactions on Electromagnetic Computations,* Vol. 36, No. 3, 189–195, August 1994.

6. Pierri, R., G. D'Elia, and F. Soldovieri, "A two probes scanning phaseless near-field far-field transformation technique," *IEEE Transactions on Antennas and Propagation,* Vol. 47, 792–802, May 1999.

7. Bucci, O. M., G. D'Elia, and M. D. Migliore, "An effective near-field far-field transformation technique from truncated and inaccurate amplitude-only data," *IEEE Transactions on Antennas and Propagation,* Vol. 47, 1377–1385, September 1999.

8. McNay, D., E. Michielssen, R. L. Rogers, S. A. Taylor, M. Akhtari, and W. W. Sutherling, "Multiple source localization using genetic algorithms," *J. Neurosci. Methods,* Vol. 64, 163–172, February 1996.

9. Regue, J. R., M. Ribo, J. M. Garrell, S. Sorroche, and J. Ayuso, "A genetic algorithm based method for predicting far-field emissions from near-field measurements," *Proceedings 2000 IEEE EMC Symposium,* 147–151, Washington, DC, August 21–25, 2000.

10. Regue, J. R., M. Ribo, J. M. Garrell, and A. Martin, "A genetic algorithm based method for source identification and far-field radiated emissions prediction from near-field measurements for PCB characterization," *IEEE Transactions on Electromagnetic Compatability,* Vol. 43, No. 4, 520–530, November 2001.

11. WIPL-D — A General-Purpose Electromagnetic Simulator for Electromagnetic Modeling of Composite Metallic and Dielectric Structures.

12. Goldberg, D. E., *Genetic Algorithms in Search, Optimization and Machine Learning,* Addison-Wesley, Reading, MA, 1989.

13. Rahmat-Samii, Y. and E. Michielssen, *Electromagnetic Optimization by Genetic Algorithms,* John Wiley & Sons, Inc., 1999

14. Linden, D. S., "Automated design and optimization of wire antennas using genetic algorithms," Ph.D. Thesis, MIT, September 1997.

15. http:Mancet.mit.edu/~mbwall/presentations/lntroToGAs/P002.html

16. http://cs.felk.cvut.cz/~xobitko/ga

17. Haupt, R. L. and S. E. Haupt, *Practical Genetic Algorithms,* John

Wiley & Sons Inc., 1998.

Taninder S. Sijher was born in Jalandhar, India on September 14th, 1979. He completed his junior high from St. Joseph Convent School in Phagwara, India and his high school from D.A.V. College Amritsar, India. After high school he joined Indian Institute of Technology, Bombay for his undergraduate degree in Electrical Engineering and received his Bachelors in July 2001. Later he joined the University of Mississippi in August 2001 for M.S. in Electrical Engineering, completing the degree in May 2004. He is currently working for Intel Corporation.

Ahmed A. Kishk joined the Department of Electrical Engineering, University of Mississippi, in 1986. He is now a Professor at the University of Mississippi and an Editor of *Antennas & Propagation Magazine*. He was an Editor-in-Chief of the *Applied Electromagntics and Computational Society Journal* from 1998 to 2001. His research interest includes the areas of design of millimeter frequency antennas, feeds for parabolic reflectors, dielectric resonator antennas, microstrip antennas, soft and hard surfaces, phased array antennas, and computer aided design for antennas. He has published 200 refereed Journal articles and over 260 proceeding papers, conference, technical reports, book chapters, and patents. He is a coauthor of the *Microwave Horns and Feeds* book (London, UK, EE, 1994; New York: EEE, 1994) and a coauthor of chapter 2 on *Handbook of Microstrip Antennas* (Peter Peregrinus Limited, United Kingdom, J. R. James and P. S. Hall (eds.), Ch. 2, 1989). He received the 1995 outstanding paper award for a paper published in the Applied Computational Electromagnetic Society Journal. He is the recipient of several awards. The latest is the Microwave Theory and Techniques Society Microwave Prize 2004. He is a Fellow member of IEEE.